

Optimization of Nylon 6 Reactors with End-Point Constraints

SANTOSH K. GUPTA, * B. S. DAMANIA, and ANIL KUMAR,
*Department of Chemical Engineering, Indian Institute of Technology,
Kanpur-208016, India*

Synopsis

Optimal temperature profiles for nylon 6 polymerization in plug-flow reactors have been obtained with end-point constraints involving the degree of polymerization and the cyclic dimer concentration, using the most recent kinetic information. Computations suggest that the temperature at the feed end of the reactor must be maintained close to the highest permissible level (determined by the boiling point of the ϵ -caprolactam). The temperatures in this region control the degree of polymerization more than other variables. Thereafter, the temperature should be reduced. This second zone controls the undesirable cyclic dimer concentration. The effect of a systematic change of values of the various design variables is studied. The profiles obtained herein are qualitatively similar to those obtained by earlier workers using similar formulations. However, they differ significantly from the profiles obtained by us earlier, using different objective functions which are more relevant to the design of *new* reactors. Attempts have also been made to obtain a global optimal scheme to produce polymer of a desired degree of polymerization and cyclic dimer content, using as short a reactor as possible, and using the water content and the modifier concentration in the feed as the independent variables.

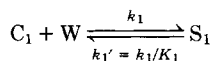
INTRODUCTION

The manufacture of nylon 6 by the hydrolytic polymerization of ϵ -caprolactam is an important industrial process. In recent years, a considerable amount of published information has appeared¹⁻¹⁸ on the detailed modeling and numerical simulation of the various industrial reactors used for the production of this polymer. These advances in the polymerization reaction engineering of nylon 6 have proceeded along several directions, some of which include the detailed description of the rates of various reactions¹⁻¹² including various side reactions leading to undesirable cyclic products, the effect of the various physical processes taking place in the reactor, as, for example, mixing of fluid elements,^{4,9,13-17,19} mass transfer of the condensation product out of the reaction mass,^{16,20,21} heat transfer through the relatively low conducting reaction mass to the heating and cooling surfaces,^{9,18} and the optimization of reactors and reactor sequences.^{4,22-25} These studies have been discussed in detail in recent review articles.^{26,27} Though a sufficient amount of information is available on the kinetics of the reaction, several problems still need to be studied in the area of transport (physical) processes as operative in various industrial reactors. In addition, much more work on the optimization of these reactors needs to be done, both when these transport processes are appropriately modeled, as also when they are assumed to be unimportant. This paper attempts to obtain optimal temperature profiles in tu-

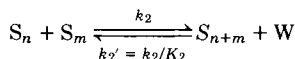
* To whom correspondence should be addressed.

TABLE I
 Kinetic Scheme and Data⁵⁻⁹ for Nylon 6 Polymerization^a

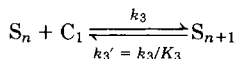
1. Ring opening



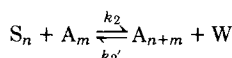
2. Polycondensation



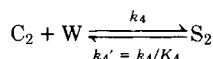
3. Polyaddition



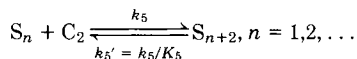
4. Reaction with monofunctional acid



5. Ring opening of cyclic dimer



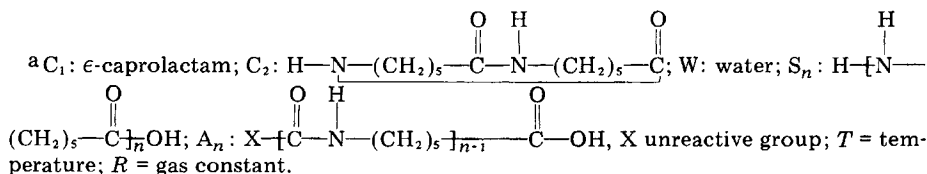
6. Polyaddition of cyclic dimer



Rate and equilibrium constants

$$\begin{aligned}
 k_i &= A_i^0 \exp\left(-\frac{E_i^0}{RT}\right) + A_i^c \exp\left(-\frac{E_i^c}{RT}\right) \sum_{n=1}^{\infty} ([A_n] + [S_n]) \\
 &= k_i^0 + k_i^c \sum_{n=1}^{\infty} ([S_n] + [A_n]) \\
 K_i &= \exp\left[\frac{\Delta S_i - \Delta H_i/T}{R}\right], i = 1, 2, \dots, 5
 \end{aligned}$$

<i>i</i>	A_i^0 (kg/mol-h)	E_i^0 (cal/mol)	A_i^c (kg ² /mol ² -h)	E_i^c (cal/mol)	ΔH_i (cal/mol)	ΔS_i (eu)
1	5.9874×10^5	1.9880×10^4	4.3075×10^7	1.8806×10^4	1.9180×10^3	-7.8846×10^0
2	1.8942×10^{10}	2.3271×10^4	1.2114×10^{10}	2.0670×10^4	-5.9458×10^3	9.4374×10^{-1}
3	2.8558×10^9	2.2845×10^4	1.6377×10^{10}	2.0107×10^4	-4.0438×10^3	-6.9457×10^0
4	8.5778×10^{11}	4.2000×10^4	2.3307×10^{12}	3.7400×10^4	-9.6000×10^3	-1.4520×10^1
5	2.5701×10^8	2.1300×10^4	3.0110×10^9	2.0400×10^4	-3.1691×10^3	5.8265×10^{-1}



bular reactors in which the transport processes are assumed to be rapid so that the rates of polymerization are determined purely by the kinetics of the reaction. It may be emphasized that this assumption is made solely to keep the analysis simple, since heat transfer in the polymerization reactor is actually far from being rapid.

TABLE II
 Mass Balance Equations (State Variable Equations)^a

$$\begin{aligned}
 f_1 \equiv \dot{x}_1 &\equiv \frac{d[C_1]}{dt} = -k_1[C_1][W] + k'_1[S_1] - k_3[C_1]\mu_0 + k'_3(\mu_0 - [S_1]) \\
 f_2 \equiv \dot{x}_2 &\equiv \frac{d[S_1]}{dt} = k_1[C_1][W] - k'_1[S_1] - 2k_2[S_1]\mu_0 + 2k'_2[W](\mu_0 - [S_1]) \\
 &\quad - k_3[S_1][C_1] + k'_3[S_2] - k_2\mu'_0[S_1] + k'_2[W](\mu'_0 - [A_1]) \\
 &\quad - k_5[S_1][C_2] + k'_5[S_3] \\
 f_3 \equiv \dot{x}_3 &\equiv \frac{d\mu_0}{dt} = k_1[C_1][W] - k'_1[S_1] - k_2\mu_0^2 + k'_2[W](\mu_1 - \mu_0) - k_2\mu_0\mu'_0 \\
 &\quad + k'_2[W](\mu'_1 - \mu'_0) + k_4[W][C_2] - k'_4[S_2] \\
 f_4 \equiv \dot{x}_4 &\equiv \frac{d\mu_1}{dt} = k_1[C_1][W] - k'_1[S_1] + k_3[C_1]\mu_0 - k'_3(\mu_0 - [S_1]) \\
 &\quad - k_2\mu'_0\mu_1 - k'_2[W]\left(\frac{\mu'_1 - \mu'_2}{2}\right) + 2k_5[C_2]\mu_0 \\
 &\quad - 2k'_5(\mu_0 - [S_1] - [S_2]) + 2k_4[W][C_2] - 2k'_4[S_2] \\
 f_5 \equiv \dot{x}_5 &\equiv \frac{d\mu_2}{dt} = k_1[C_1][W] - k'_1[S_1] + 2k_2\mu_1^2 + \frac{k'_2}{3}[W](\mu_1 - \mu_3) \\
 &\quad + k_3[C_1](\mu_0 + 2\mu_1) + k'_3(\mu_0 - 2\mu_1 + [S_1]) \\
 &\quad - k_2\mu_2\mu'_0 + \frac{k'_2}{6}[W](2\mu'_3 - 3\mu'_2 + \mu'_1) \\
 &\quad + 4k_5[C_2](\mu_1 + \mu_0) + 4k'_5(\mu_0 - \mu_1 + [S_2]) + 4k_4[W][C_2] - 4k'_4[S_2] \\
 f_6 \equiv \dot{x}_6 &\equiv \frac{d[C_2]}{dt} = -k_4[C_2][W] + k'_4[S_2] - k_5[C_2]\mu_0 + k'_5(\mu_0 - [S_1] - [S_2]) \\
 f_7 \equiv \dot{x}_7 &\equiv \frac{d[W]}{dt} = -k_1[C_1][W] + k'_1[S_1] + k_2(\mu_0)^2 - k'_2[W](\mu_1 - \mu_0) \\
 &\quad + k_2\mu_0\mu'_0 - k'_2[W](\mu'_1 - \mu'_0) - k_4[C_2][W] + k'_4[S_2] \\
 f_8 \equiv \dot{x}_8 &\equiv \frac{d\mu'_1}{dt} = k_2\mu_1\mu'_0 - \frac{k'_2[W]}{2}(\mu'_2 - \mu'_1) \\
 f_9 \equiv \dot{x}_9 &\equiv \frac{d\mu'_2}{dt} = k_2(2\mu_1\mu'_1 + \mu_2\mu'_0) - \frac{k'_2[W]}{6}(4\mu'_3 - 3\mu'_2 - \mu'_1) \\
 f_{10} \equiv \dot{x}_{10} &\equiv \frac{d[A_1]}{dt} = -k_2[A_1]\mu_0 + k'_2[W](\mu'_0 - [A_1])
 \end{aligned}$$

Closure conditions,^{8,16,20} $[S_2] = [S_3] = [S_1]$

$$\mu_3 = \frac{\mu_2(2\mu_2\mu_0 - \mu_1^2)}{\mu_1\mu_0}, \quad \mu'_3 = \frac{\mu'_2(2\mu'_2\mu'_0 - \mu_1'^2)}{\mu'_1\mu'_0}$$

^a $\mu_k \equiv \sum_{n=1}^{\infty} n^k [S_n]$, $\mu'_k \equiv \sum_{n=1}^{\infty} n^k [A_n]$, $k = 0, 1, 2, 3$, $d\mu'_0/dt = 0$ or $\mu'_0 = \text{const}$ (= inlet value).

The first detailed optimization of nylon 6 reactors was studied by Hoftzyer et al.,²² who used dynamic programming to obtain the optimal temperature and water concentration profiles for producing polymer having a fixed value of the degree of polymerization \overline{DP} in as short a reactor as possible. Their study

TABLE III
Summary of the Numerical Algorithm

Objective function

$$\text{minimize } I(x_1, x_2, \dots, x_n)_{t=t_f} \\ T(t)$$

Mass balance (state variable) equations (Table II)

$$\frac{dx_i}{dt} = f_i(x_1, x_2, \dots, x_n, T), i = 1, 2, \dots, n$$

End points constraints

$$\psi_1(x_1, x_2, \dots, x_n)_{t_f} = 0, \psi_2(x_1, x_2, \dots, x_n)_{t_f} = 0$$

Constraints on T

$$T_{\min} \leq T \leq T_{\max}$$

Adjoint function equations (Table IV)

$$\frac{d\lambda_{i,j}}{dt} = - \sum_{k=1}^n \frac{\partial f_k}{\partial x_i} \lambda_{k,j} \\ i = 1, 2, \dots, n, j = 1, 2, 3 \\ \lambda_{i,1}(t_f) = \left. \frac{\partial I}{\partial x_i} \right|_{t_f}, i = 1, 2, \dots, n \\ \lambda_{i,2}(t_f) = \left. \frac{\partial \psi_1}{\partial x_i} \right|_{t_f}, i = 1, 2, \dots, n \\ \lambda_{i,3}(t_f) = \left. \frac{\partial \psi_2}{\partial x_i} \right|_{t_f}, i = 1, 2, \dots, n$$

Increment in $T(t)$ ^{30,31}

$$\delta T(t) = - \left[\frac{\partial f_1}{\partial T}, \frac{\partial f_2}{\partial T}, \dots, \frac{\partial f_n}{\partial T} \right] \\ \times \left\{ \begin{bmatrix} \lambda_{1,1} \\ \lambda_{2,1} \\ \vdots \\ \lambda_{n,1} \end{bmatrix} - \begin{bmatrix} \lambda_{1,2} & \lambda_{1,3} \\ \lambda_{2,2} & \lambda_{2,3} \\ \vdots & \vdots \\ \lambda_{n,2} & \lambda_{n,3} \end{bmatrix} \begin{bmatrix} I_{\psi_1,1}^{-1} & I_{\psi_1,2}^{-1} \\ I_{\psi_2,1}^{-1} & I_{\psi_2,2}^{-1} \\ \vdots & \vdots \end{bmatrix} \begin{bmatrix} I_{\psi_1,1} \\ I_{\psi_1,2} \end{bmatrix} \right\} \\ + \left[\frac{\partial f_1}{\partial T}, \dots, \frac{\partial f_n}{\partial T} \right] \begin{bmatrix} \lambda_{1,2} & \lambda_{1,3} \\ \vdots & \vdots \\ \lambda_{n,2} & \lambda_{n,3} \end{bmatrix} \begin{bmatrix} I_{\psi_1,1}^{-1} & I_{\psi_1,2}^{-1} \\ I_{\psi_2,1}^{-1} & I_{\psi_2,2}^{-1} \\ \vdots & \vdots \end{bmatrix} \begin{bmatrix} \delta \psi_1 \\ \delta \psi_2 \end{bmatrix}$$

showed the optimal configuration to be a sequence of two reactors, the first operating at a high temperature and high water concentration and the second operating at lower temperature and water concentration. It was assumed that instantaneous removal of water could take place in between these two reactors, something which would be physically difficult to achieve in view of the low diffusivities of water through the relatively viscous reaction mass. Hoftzyer et al., however, presented only semiquantitative results, probably because of proprietary reasons. Reimschuessel and Nagasubramanian⁴ studied combinations of a two-stage isothermal plug-flow reactor system, with water concentration as the main process parameter and presented quantitative results of their optimization. These two studies incorporated only the three major reactions (ring opening, polycondensation, and polyaddition) in the kinetic scheme. Naudin

TABLE III (Continued from the previous page.)

7with $I_{\psi,l,m}^{-1}$ ($l,m = 1,2$) being elements of a 2×2 matrix I_{ψ}^{-1} and $I_{\psi,l}$ ($l = 1,2$) being elements of a 2×1 matrix I_{ψ} given below:

$$I_{\psi\psi} \equiv \int_0^{t_f} \begin{bmatrix} \lambda_{1,2} & \lambda_{2,2} & \dots & \lambda_{n,2} \\ \lambda_{1,3} & \lambda_{2,3} & \dots & \lambda_{n,3} \end{bmatrix} \begin{bmatrix} \frac{\partial f_1}{\partial T} \\ \vdots \\ \frac{\partial f_n}{\partial T} \end{bmatrix} \begin{bmatrix} \frac{\partial f_1}{\partial T}, \dots, \frac{\partial f_n}{\partial T} \\ \vdots \\ \lambda_{n,2} & \lambda_{n,3} \end{bmatrix} dt$$

$$I_{\psi I} \equiv \int_0^{t_f} \begin{bmatrix} \lambda_{1,2} & \lambda_{2,2} & \dots & \lambda_{n,2} \\ \lambda_{1,3} & \dots & \dots & \lambda_{n,3} \end{bmatrix} \begin{bmatrix} \frac{\partial f_1}{\partial T} \\ \vdots \\ \frac{\partial f_n}{\partial T} \end{bmatrix} \begin{bmatrix} \lambda_{1,1} \\ \lambda_{2,1} \\ \vdots \\ \lambda_{n,1} \end{bmatrix} dt$$

Increments $\delta\psi_1$ and $\delta\psi_2$

$$\begin{bmatrix} \delta\psi_1 \\ \delta\psi_2 \end{bmatrix} = -\epsilon \begin{bmatrix} \psi_1(t_f) \\ \psi_2(t_f) \end{bmatrix}, \quad 0 \leq \epsilon \leq 1$$

ten Cate²³ and Mochizuki and Ito²⁴ incorporated some approximate equations for the rate of the (undesirable) cyclic oligomer formation in their kinetic scheme and obtained optimal temperature profiles required to produce nylon 6 of a fixed \overline{DP} , simultaneously controlling (minimizing²³ or attaining a fixed value²⁴ of) the total cyclic oligomers formed, as well as maximizing the caprolactam conversion. Both these groups of workers assumed no evaporation of water in their tubular reactor (which was justified because of the hydrostatic pressure head) and found that the temperature should first be increased in the flow direction and then decreased. Their optimal temperature profiles differed quantitatively because of the differences in the objective functions and in the rate expressions for cyclic oligomer formation. In addition, in both these studies, again, only semiquantitative results were presented.

It has been pointed out^{25,28,29} that several physically meaningful objective functions can be formulated in the optimization of polymerization reactors. This is partly so because a designer of a new plant has more degrees of freedom available to him than an engineer who wishes to find the optimal conditions to produce a certain product from an already installed reactor. Most^{4,22-24} of the optimization studies on nylon 6 belong to the second category, while only one recent study²⁵ pertains to the optimization of a reactor at the design stage. The optimal temperature profiles obtained for these two classes of objective functions differ significantly, both qualitatively as well as quantitatively, and this emphasizes the need for precaution in the choice of objective functions. It may be

TABLE IV
Equations for the Adjoint Functions $\lambda_{i,j}$ ($i = 1, 2, \dots, n; j = 1, 2, 3$)^a

$$\begin{aligned}
 -\frac{d\lambda_1}{dt} &= (k_1[W] + k_3\mu_0)(-\lambda_1 + \lambda_4 + \lambda_5) + k_1[W](\lambda_2 + \lambda_3 - \lambda_7) \\
 &\quad - k_3[S_1]\lambda_2 + 2k_3\mu_1\lambda_5 \\
 -\frac{d\lambda_2}{dt} &= \frac{k_1}{K_1}(\lambda_1 - \lambda_2 - \lambda_3 - \lambda_4 - \lambda_5 + \lambda_7) + \frac{k_3}{K_3}(-\lambda_1 + \lambda_4 + \lambda_5) \\
 + \frac{k_5}{K_5}(2\lambda_4 - \lambda_6) + \lambda_2(-2k_2\mu_0 - 2\frac{k_2}{K_2}[W] - k_2\mu'_0 - k_3[C_1] - k_5[C_2]) \\
 -\frac{d\lambda_3}{dt} &= \left(k_3[C_1] - \frac{k_3}{K_3}\right)(-\lambda_1 + \lambda_4) + \left(k_3[C_1] + \frac{k_3}{K_3}\right)(\lambda_5) \\
 + \left(k_2[S_1] - \frac{k_2}{K_2}[W]\right)(-2\lambda_2) + \left(2k_2\mu_0 + \frac{k_2}{K_2}[W] + k_2\mu'_0\right)(-\lambda_3 + \lambda_7) \\
 + \left(k_5[C_2] - \frac{k_5}{K_5}\right)(2\lambda_4 - \lambda_6) + \left(k_5[C_2] + \frac{k_5}{K_5}\right)(4\lambda_5) - k_2[A_1]\lambda_{10} \\
 + k_1^c \left([C_1][W] - \frac{[S_1]}{K_1}\right)(-\lambda_1 + \lambda_2 + \lambda_3 + \lambda_4 + \lambda_5 - \lambda_7) \\
 + k_2^c \left(\mu_0^2 + \mu_0\mu'_0 - \frac{[W](\mu_1 - \mu_0)}{K_2} - \frac{[W](\mu'_1 - \mu'_0)}{K_2}\right)(-\lambda_3 + \lambda_7) \\
 + k_3^c \left(\mu_0[C_1] - \frac{\mu_0 - [S_1]}{K_3}\right)(-\lambda_1 + \lambda_4) \\
 + k_4^c \left([W][C_2] - \frac{[S_2]}{K_4}\right)(\lambda_3 + 2\lambda_4 + 4\lambda_5 - \lambda_6 - \lambda_7) \\
 - 2k_5^c\lambda_2 \left(\mu_0[S_1] - \frac{[W](\mu_0 - [S_1])}{K_2} + \frac{\mu'_0[S_1]}{2} - [W]\frac{(\mu'_0 - [A_1])}{2K_2}\right) \\
 - k_5^c\lambda_4 \left(\mu_1\mu'_0 + \frac{[W](\mu'_1 - \mu'_2)}{2K_2}\right) + 2k_5^c\lambda_5 \left(\mu_1^2 + [W]\frac{(\mu_1 - \mu_3)}{6K_2}\right) \\
 - k_5^c\lambda_5 \left(\mu_2\mu'_0 - \frac{[W](2\mu'_3 - 3\mu'_2 + \mu'_1)}{6K_2}\right) + k_5^c\lambda_8 \left(\mu_1\mu'_0 - \frac{[W](\mu'_2 - \mu'_1)}{2K_2}\right) \\
 + k_5^c\lambda_9 \left(2\mu_1\mu'_1 + \mu_2\mu'_0 - \frac{[W](4\mu'_3 - 3\mu'_2 - \mu'_1)}{6K_2}\right) \\
 - k_5^c\lambda_{10} \left(\mu_0[A_1] - [W]\frac{\mu'_0 - [A_1]}{K_2}\right) - k_5^c\lambda_2 \left([C_1][S_1] - \frac{[S_2]}{K_3}\right) \\
 + k_5^c\lambda_5 \left((\mu_0 + 2\mu_1)[C_1] + \frac{\mu_0 - 2\mu_1 + [S_1]}{K_3}\right) \\
 - k_5^c\lambda_2 \left([S_1][C_2] - \frac{[S_3]}{K_5}\right) + k_5^c \left([C_2]\mu_0 - \frac{\mu_0 - [S_1] - [S_2]}{K_5}\right)(2\lambda_4 - \lambda_6) \\
 + 4k_5^c\lambda_5 \left([C_2](\mu_1 + \mu_0) + \frac{\mu_0 - \mu_1 + [S_2]}{K_5}\right) \\
 -\frac{d\lambda_4}{dt} &= \frac{k_2[W]}{K_2} \left(\lambda_3 + \frac{\lambda_5}{3} - \lambda_7\right) + k_2\mu'_0(-\lambda_4 + \lambda_8) \\
 + \left(2k_3[C_1] - 2\frac{k_3}{K_3} + 4k_5[C_2] - \frac{4k_5}{K_5} + 4k_2\mu_1\right)\lambda_5 + 2k_2\mu'_1\lambda_9 \\
 -\frac{d\lambda_5}{dt} &= k_2\mu'_0(\lambda_9 - \lambda_5) \\
 -\frac{d\lambda_6}{dt} &= k_4[W](\lambda_3 + 2\lambda_4 + 4\lambda_5 - \lambda_6 - \lambda_7) + k_5\mu_0(2\lambda_4 + 4\lambda_5 - \lambda_6)
 \end{aligned}$$

TABLE IV (Continued from the previous page.)

$$\begin{aligned}
 & -k_5[S_1]\lambda_2 + 4k_5\mu_1\lambda_5 \\
 -\frac{d\lambda_7}{dt} = & k_1[C_1](-\lambda_1 + \lambda_2 + \lambda_3 + \lambda_4 + \lambda_5 - \lambda_7) + k_4[C_2](\lambda_3 + 2\lambda_4 + 4\lambda_5 - \lambda_6 - \lambda_7) \\
 & + \frac{k_2}{K_2}(\mu_1 - \mu_0)(\lambda_3 - \lambda_7) + \frac{k_2}{K_2}(\mu'_1 - \mu'_0)(\lambda_3 - \lambda_7) \\
 & + \frac{k_2}{K_2} \left\{ 2(\mu_0 - [S_1])\lambda_2 + (\mu'_0 - [A_1])(\lambda_2 + \lambda_{10}) - \frac{(\mu'_1 - \mu'_2)}{2}(\lambda_4 - \lambda_8) \right. \\
 & \left. + \frac{(\mu_1 - \mu_3)}{3}\lambda_5 + \frac{(2\mu'_3 - 3\mu'_2 + \mu'_1)}{6}\lambda_5 - \frac{4\mu'_3 - 3\mu'_2 - \mu'_1}{6}\lambda_9 \right\} \\
 -\frac{d\lambda_8}{dt} = & \frac{k_2}{K_2}[W] \left(\lambda_3 - \frac{\lambda_4}{2} + \frac{\lambda_5}{6} - \lambda_7 + \frac{\lambda_8}{2} + \frac{\lambda_9}{6} \right) + 2k_2\mu_1\lambda_9 \\
 & - \frac{d\lambda_9}{dt} = \frac{k_2[W]}{2K_2}(\lambda_4 - \lambda_5 - \lambda_8 + \lambda_9) \\
 -\frac{d\lambda_{10}}{dt} = & \frac{k_2[W]}{K_2}(-\lambda_2 - \lambda_{10}) - k_2\mu_0\lambda_{10}
 \end{aligned}$$

Boundary conditions

$$\begin{aligned}
 \lambda_{1,1}(t_f) &= 2[C_1]_{t_f} \\
 \lambda_{4,2}(t_f) &= 1 \\
 \lambda_{8,2}(t_f) &= 1 \\
 \lambda_{3,2}(t_f) &= -\overline{DP}_d \\
 \lambda_{6,3}(t_f) &= 1 \\
 \text{all other } \lambda_{i,j}(t_f) &= 0
 \end{aligned}$$

^a In the equations, the subscript j on the $\lambda_{i,j}$ has been omitted for brevity.

added that Ray and Szekely²⁸ and Denn²⁹ have compiled several optimization case studies for nonpolymeric reactors which demonstrate the effect of the objective function on the optimal temperature profiles.

In this paper we carry out a detailed optimization study using an objective function of the first type discussed above, namely, one relevant to an operating plant. The objective function is similar to that used by Mochizuki and Ito.²⁴ However, there are two important differences. The first is that a more appropriate expression for the rate of cyclic oligomer formation developed recently by Tai et al.⁵⁻¹⁰ has been used. The other is that *detailed quantitative* effects of the various independent variables (e.g., time of reaction, initial or feed water content, monofunctional acid concentration in feed, etc.) have been presented. In addition, a simple, first-order mathematical technique called the modified control vector iteration method has been used which takes less computational time and effort compared to the second-order techniques used in earlier studies. The results obtained are found to be qualitatively similar to those of earlier workers²²⁻²⁴ using similar objective functions.

FORMULATION

The kinetic scheme used in this work is given in Table I along with the rate

TABLE V
Expressions for $\partial f_i / \partial T$

$$\begin{aligned} \frac{\partial f_1}{\partial T} &= -k_1^* \left([W][C_1] - \frac{[S_1]}{K_1} \right) - \frac{k_1 K_1^*}{K_1^2} [S_1] - k_3^* \left(\mu_0 [C_1] - \frac{\mu_0 - [S_1]}{K_3} \right) \\ &\quad - \frac{k_3 K_3^*}{K_3^2} (\mu_0 - [S_1]) \\ \frac{\partial f_2}{\partial T} &= k_1^* \left([W][C_1] - \frac{[S_1]}{K_1} \right) + \frac{k_1 K_1^*}{K_1^2} [S_1] - 2k_2^* \left(\mu_0 [S_1] - \frac{[W](\mu_0 - [S_1])}{K_2} \right) \\ &\quad + \frac{\mu_0' [S_1]}{2} - \frac{[W](\mu_0' - [A_1])}{2K_2} \Big) - \frac{2k_2 K_2^* [W]}{K_2^2} \left(\mu_0 - [S_1] + \frac{\mu_0' - [A_1]}{2} \right) \\ &\quad - k_3^* \left([C_1][S_1] - \frac{[S_2]}{K_3} \right) - \frac{k_3 K_3^*}{K_3^2} [S_2] - k_5^* \left([C_2][S_1] - \frac{[S_3]}{K_5} \right) \\ &\quad - \frac{k_5 K_5^*}{K_5^2} [S_3] \\ \frac{\partial f_3}{\partial T} &= k_1^* \left([W][C_1] - \frac{[S_1]}{K_1} \right) + \frac{k_1 K_1^*}{K_1^2} [S_1] - k_2^* \left(\mu_0^2 - \frac{[W](\mu_1 - \mu_0)}{K_2} \right) \\ &\quad + \mu_0 \mu_0' - \frac{[W](\mu_1' - \mu_0')}{K_2} \Big) - \frac{k_2 K_2^*}{K_2^2} [W](\mu_1 + \mu_1' - \mu_0 - \mu_0') \\ &\quad + k_4^* \left([W][C_2] - \frac{[S_2]}{K_4} \right) + \frac{k_4 K_4^*}{K_4^2} [S_2] \\ \frac{\partial f_4}{\partial T} &= k_1^* \left([W][C_1] - \frac{[S_1]}{K_1} \right) + \frac{k_1 K_1^*}{K_1^2} [S_1] + k_3^* \left(\mu_0 [C_1] - \frac{\mu_0 - [S_1]}{K_3} \right) \\ &\quad + \frac{k_3 K_3^*}{K_3^2} (\mu_0 - [S_1]) + 2k_4^* \left([W][C_2] - \frac{[S_2]}{K_4} \right) + \frac{2k_4 K_4^*}{K_4^2} [S_2] \\ &\quad + 2k_5^* \left(\mu_0 [C_2] - \frac{\mu_0 - [S_1] - [S_2]}{K_5} \right) + \frac{2k_5 K_5^*}{K_5^2} (\mu_0 - [S_1] - [S_2]) \\ &\quad - k_2^* \left(\mu_0' \mu_1 + \frac{[W](\mu_1' - \mu_2')}{2K_2} \right) + \frac{k_2 K_2^*}{2K_2^2} [W](\mu_1' - \mu_2') \\ \frac{\partial f_5}{\partial T} &= k_1^* \left([W][C_1] - \frac{[S_1]}{K_1} \right) + \frac{k_1 K_1^*}{K_1^2} [S_1] + \frac{k_2^* [W](\mu_1 - \mu_3)}{3K_2} \\ &\quad - \frac{k_2 K_2^*}{3K_2^2} (\mu_1 - \mu_3) + k_3^* \left([C_1](2\mu_1 + \mu_0) + \frac{\mu_0 - 2\mu_1 + [S_1]}{K_3} \right) \\ &\quad - \frac{k_3 K_3^*}{K_3^2} (\mu_0 - 2\mu_1 + [S_1]) + 4k_5^* \left([C_2](\mu_0 + \mu_1) \right. \\ &\quad \left. + \frac{\mu_0 - \mu_1 + [S_2]}{K_5} \right) - \frac{4k_5 K_5^*}{K_5^2} (\mu_0 - \mu_1 + [S_2]) \\ &\quad + 4k_4^* \left([W][C_2] - \frac{[S_2]}{K_4} \right) + \frac{4k_4 K_4^*}{K_4^2} [S_2] \\ &\quad + k_2^* \left(2\mu_1^2 - \mu_2 \mu_0' + \frac{[W](2\mu_3' - 3\mu_2' + \mu_1')}{6K_2} \right) - \frac{k_2 K_2^*}{6K_2^2} [W](2\mu_3' - 3\mu_2' + \mu_1') \\ \frac{\partial f_6}{\partial T} &= -k_4^* \left([W][C_2] - \frac{[S_2]}{K_4} \right) - \frac{k_4 K_4^*}{K_4^2} [S_2] - k_5^* \left(\mu_0 [C_2] - \frac{\mu_0 - [S_1] - [S_2]}{K_5} \right) \\ &\quad - \frac{k_5 K_5^*}{K_5^2} (\mu_0 - [S_1] - [S_2]) \\ \frac{\partial f_7}{\partial T} &= -k_1^* \left([W][C_1] - \frac{[S_1]}{K_1} \right) - \frac{k_1 K_1^*}{K_1^2} [S_1] + k_2^* \left(\mu_0^2 - \frac{[W](\mu_1 - \mu_0)}{K_2} \right) + \mu_0 \mu_0' \\ &\quad - \frac{[W](\mu_1' - \mu_0')}{K_2} \Big) + \frac{k_2 K_2^*}{K_2^2} [W](\mu_1 - \mu_0 + \mu_1' - \mu_0') \end{aligned}$$

TABLE V (Continued from the previous page.)

$$\begin{aligned}
 & -k_4^* \left([W][C_2] - \frac{[S_2]}{K_4} \right) - \frac{k_4 K_4^*}{K_4^2} [S_2] \\
 \frac{\partial f_8}{\partial T} &= k_2^* \left(\mu_1 \mu'_0 - \frac{[W](\mu'_2 - \mu'_1)}{2K_2} \right) + \frac{k_2 K_2^*}{2K_2^2} [W](\mu'_2 - \mu'_1) \\
 \frac{\partial f_9}{\partial T} &= k_2^* \left(2\mu_1 \mu'_1 + \mu_2 \mu'_0 - \frac{[W](4\mu'_3 - 3\mu'_2 - \mu'_1)}{6K_2} \right) \\
 & \quad + \frac{k_2 K_2^*}{6K_2^2} [W](4\mu'_3 - 3\mu'_2 - \mu'_1) \\
 \frac{\partial f_{10}}{\partial T} &= k_2^* \left(-\mu_0 [A_1] + \frac{[W](\mu'_0 - [A_1])}{K_2} \right) - \frac{k_2 K_2^*}{K_2^2} [W](\mu'_0 - [A_1])
 \end{aligned}$$

where

$$k_i^* \equiv \frac{\partial k_i}{\partial T} = \frac{E_i^0 k_i^0 + E_i^c k_i^c (\mu_0 + \mu'_0)}{RT^2}, i = 1, 2, \dots, 5$$

and

$$K_i^* \equiv \frac{\partial K_i}{\partial T} = \frac{K_i (\Delta H_i)}{RT^2}, i = 1, 2, \dots, 5$$

and equilibrium constants.⁵⁻⁹ This represents the most recent and precise information on nylon 6 polymerization available in the literature. In addition to the three major reactions, ring-opening, polycondensation, and polyaddition, it also incorporates the reaction with monofunctional acid stabilizers and also two reactions involving the cyclic dimer. The reactions with higher cyclic oligomers are not incorporated in this scheme since equally precise rate constants are not available. Recently there has been a study¹⁰ which presents experimental data on the buildup of various cyclic oligomers with time and which can be used to obtain the rate constants. However, since it is well established that the cyclic dimer constitutes the major share of the cyclic compounds in the reaction mass, very little error is expected because of this assumption. The corresponding mass balance equations are given in Table II. The balance equations require approximations to "close" the hierarchy of equations and the closure conditions used by Tai et al.⁸ are also included in this table. These closure equations have been demonstrated to be extremely successful in predicting the moments for both batch (or plug-flow) reactors²⁰ as well as for continuous-flow stirred-tank reactors¹⁶ and give results which match very well with those obtained from a detailed integration of mass balance equations of the individual species.^{14,15} The mass balance equations can be alternatively written in terms of variables used conventionally in the field of optimization.²⁸⁻³¹ For example, one can define a column vector, \mathbf{x} , of 10 state variables x_1, x_2, \dots, x_{10} , as

$$\mathbf{x} = [x_1, x_2, \dots, x_{10}]^T \equiv [[C_1], [S_1], \mu_0, \mu_1, \mu_2, [C_2], [W], \mu'_1, \mu'_2, [A_1]]^T \quad (1)$$

where T represents the transpose of the matrix and μ_i and μ'_i represent the i th moments of the bifunctional (S_n) and monofunctional (A_n) molecules. C_1, W and C_2 represent caprolactam, water, and the cyclic dimer, respectively. The equations in Table II thus represent dx_i/dt or equivalently, \dot{x}_i or f_i .

In this work, the temperature history $T(t)$ in a batch reactor, or the temperature profile in a plug-flow reactor (where t is the time taken by a fluid element

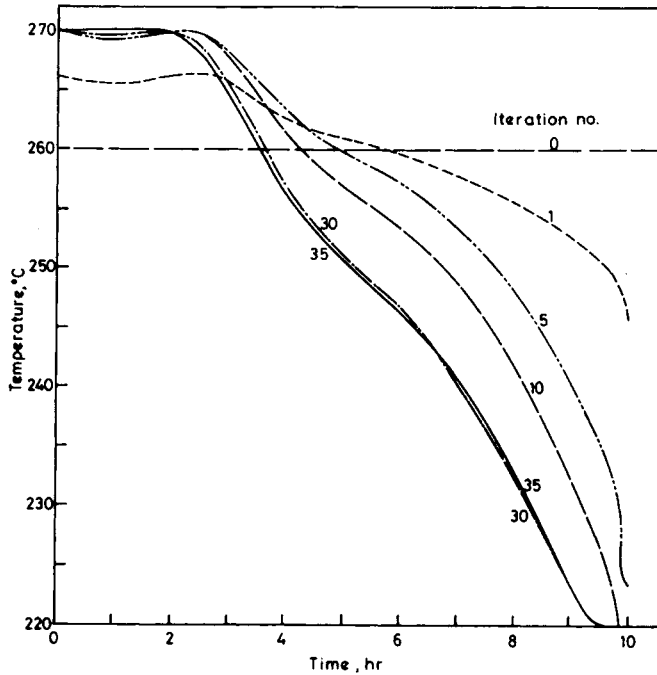


Fig. 1. Change of temperature profile with the number of iterations. Reference conditions [eq. (6)] used, $\epsilon = 0.0013$.

to reach any position) is to be so determined that an objective function $I(x_1, x_2, \dots, x_{10})_{t=t_f}$ is minimized. In this work, the following objective function is selected:

$$\text{minimize}_{T(t)} I(x_1, x_2, \dots, x_{10}) \equiv [C_1]_{t=t_f}^2 \tag{2}$$

where t_f is the total reaction or residence time, assumed to be fixed. The choice

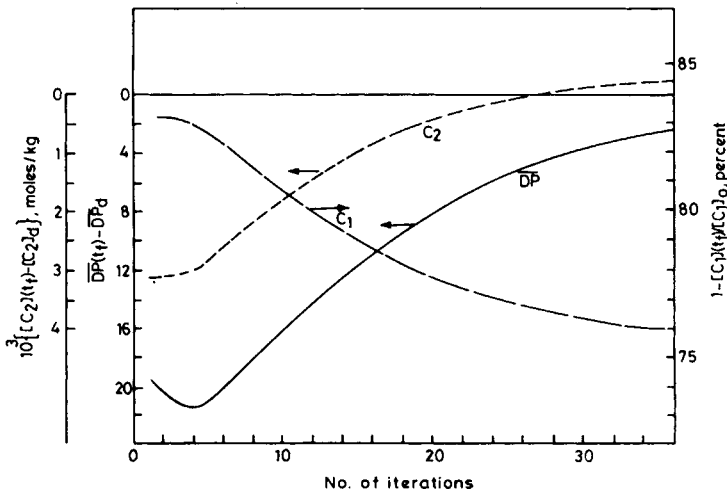


Fig. 2. Variation of ψ 's and I with the number of iterations for the reference ψ run, $\epsilon = 0.0013$.

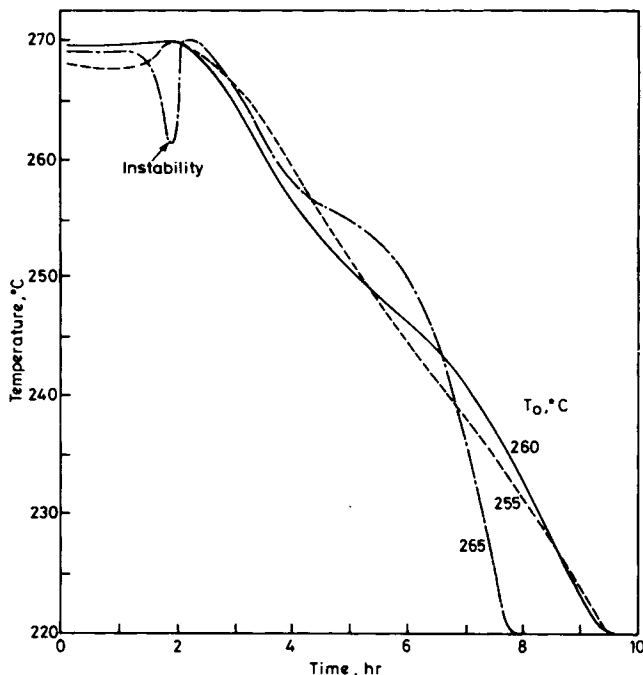


Fig. 3. Variation of the optimal temperature profile with the guess temperature T_0 . Values of ϵ , $\overline{DP}(t_f)$, $[C_2](t_f)$ (mol/kg) and conversion (%) are: at $T_0 = 255^\circ\text{C}$: 0.0001–0.005, 141.93, 0.00975, 75.65; at $T_0 = 260^\circ\text{C}$: 0.0013, 142.5, 0.00979, 75.87; at $T_0 = 265^\circ\text{C}$: 0.0001–0.01, 141.54, 0.00978, 75.59.

of I as in eq. (2) minimizes the concentration of the caprolactam C_1 at the end or exit of the reactor, and thus maximizes the monomer conversion. The optimization must be carried out subject to the following two end-point constraints

$$\psi_1 \equiv (\mu_1 + \mu'_1)_{t=t_f} - \overline{DP}_d(\mu_0 + \mu'_0)_{t=t_f} = 0 \quad (3a)$$

$$\psi_2 \equiv [C_2]_{t=t_f} - [C_2]_d = 0 \quad (3b)$$

The first of these constraints forces the degree of polymerization of the product $\{= (\mu_1 + \mu'_1)/(\mu_0 + \mu'_0)_{t=t_f}\}$ to be exactly equal to a desired value, \overline{DP}_d , while the second constraint in eq. (3) forces the cyclic dimer concentration in the product, $[C_2]_{t=t_f}$ to be equal to a desired value $[C_2]_d$. The optimization problem being solved is thus similar to that of Mochizuki and Ito.²⁴

The solution of a general optimization problem with n state variables x_1, x_2, \dots, x_n and a single control variable, T , with two end-point constraints, is summarized in Table III.^{30,31} Three sets of adjoint functions, $\lambda_{i,1}(t)$, $\lambda_{i,2}(t)$, and $\lambda_{i,3}(t)$ ($i = 1, 2, \dots, n$) must be defined. The equations for these three functions are identical in form and are given in Table III, along with "boundary conditions" at $t = t_f$. The values of these adjoint functions at any time, t , will differ since their boundary conditions are different. Table IV gives a detailed listing of these adjoint functions.

The modified control vector iteration technique of obtaining the optimal temperature profile consists of first assuming a temperature history $T(t)$ (usually taken as a constant), and then updating $T(t)$ by an increment $\delta T(t)$ given in

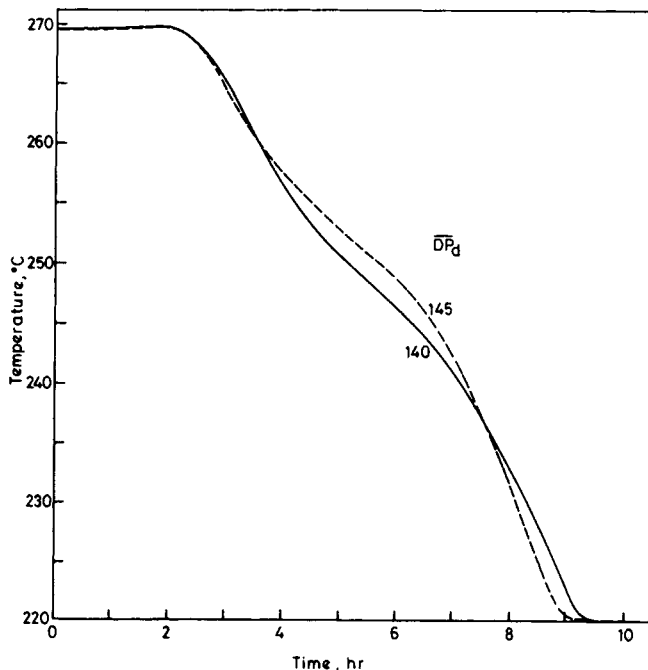


Fig. 4. Variation of the optimal temperature profile with \overline{DP}_d : (---) $\overline{DP}(t_f) = 145.07$, $[C_2](t_f) = 0.0101$, conversion $(t_f) = 76.74\%$, $\epsilon = 0.0001-0.005$; (—) reference condition.

terms of some integrals by equations in Table III.^{30,31} The various expressions for $\partial f_i/\partial T (= \partial \dot{x}_i/\partial T)$ are given in Table V. The choice of the increments $\delta\psi_1$ and $\delta\psi_2$ is made such that the numerical algorithm is forced toward $\psi_1(t_f) = 0$ and $\psi_2(t_f) = 0$, the choice of ϵ being somewhat arbitrary.

In obtaining the various equations in Tables IV and V, the closure equations of Table II have *not* been substituted in the equations for f_i while differentiating them with respect to x_j (to obtain $d\lambda_{i,j}/dt$). Thus, in computing df_5/dx_2 for example, $\partial[S_2]/\partial[S_1]$ has been taken as zero instead of unity. It is expected that differentiation after substitution of the closure equations will not give substantially different results. A similar assumption has been made earlier.²⁵

In obtaining the optimal temperature profiles, the control variable (temperature) is constrained to lie between two limiting values²²

$$220^\circ\text{C} \leq T \leq 270^\circ\text{C} \quad (4)$$

The lower of these values represents the melting point of the polymer, and the upper limit represents the approximate boiling point of (pure) caprolactam at atmospheric conditions.

In order to obtain the optimal temperature profile, the following detailed procedure as described by Bryson and Ho³¹ is used. One assumes a temperature profile $T_0(t)$, integrates the state variable equations (Table II) in the forward direction (from $t = 0$ to t_f , storing the values of $x_1, x_2, \dots, x_{10}, \partial f_1/\partial T, \dots, \partial f_{10}/\partial T$), computes the objective function, $\psi_1(t_f)$ and $\psi_2(t_f)$ (and then $\delta\psi_1, \delta\psi_2$) and the values of the adjoint functions $\lambda_{i,j}$ at $t = t_f$, integrates the adjoint function equations (Table IV) in the reverse direction (from t_f to 0), and finally

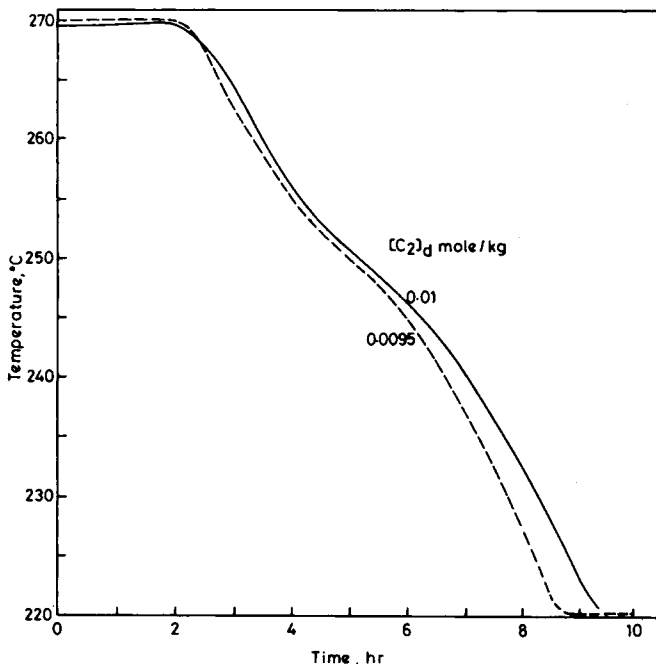


Fig. 5. Variation of the optimal temperature profile with $[C_2]_d$: (---) $\overline{DP}(t_f) = 140.13$, $[C_2](t_f) = 0.00952$ mol/kg, conversion $(t_f) = 75.04\%$, $\epsilon = 0.0001-0.005$; (—) reference run.

corrects the temperature profile using the equation for $\delta T(t)$ in Table III and

$$T^{(\text{new})}(t) = T^{(\text{old})}(t) + \delta T(t) \quad (5)$$

keeping in mind eq. (4) (in which case, the temperature is selected as the constraint value). This completes one iteration of computation. The fourth-order Runge-Kutta method is used for integration and the computations are continued till $\psi_1(t_f)$ and $\psi_2(t_f)$ are within some tolerance range and the objective function I does not change too much.

The value of Δt used for integration is chosen such that there are 231 intervals between $0 \leq t \leq t_f$. In order to reduce memory storage requirements, the values of T , λ 's and $\partial f_i / \partial T$ are stored at only 77 equally spaced points between $0 \leq t \leq t_f$ and linear interpolation is used.²⁸ Several checks were used to ensure that the results are free of errors. The computer program gave results which matched those obtained earlier^{17,20,25} under isothermal conditions. Also, independent checks on the stoichiometric balances²⁰ on $(-CH_2)_5$ units and water were made at every stage and these were found to lie within about $10^{-5}\%$ of the theoretical values. In addition, our computer program gave results identical to those obtained by Ray and Szekely²⁸ (Example 6.5.2) in the absence of end-point constraints when the corresponding equations were used. All these checks gave confidence regarding the correctness of the computer program. The computer time taken for one run involving about 50 iterations, on a DEC 1090, was approximately 5 min.

RESULTS AND DISCUSSION

A systematic parametric study was made to obtain the effect of each of the parameters on the optimal temperature profile. The following conditions used

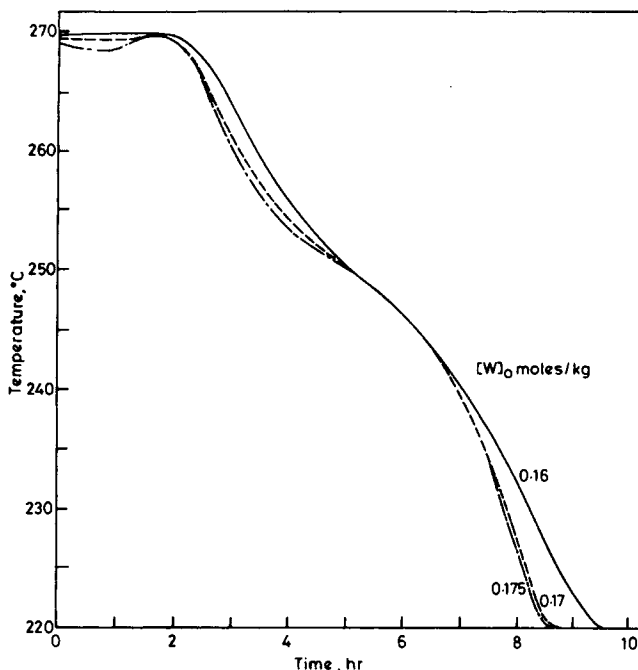


Fig. 6. Effect of changing the water concentration $[W]_0$ in the feed: (---) $[W]_0 = 0.170$ mol/kg, $\overline{DP}(t_f) = 140.394$, $[C_2](t_f) = 0.00997$; conversion = 76.98%; (-·-) $[W]_0 = 0.175$, $\overline{DP}(t_f) = 140.11$, $[C_2](t_f) = 0.0101$, conversion = 77.75%, $\epsilon = 0.0001$ – 0.002 ; (—) reference run.

earlier²⁵ were also used for the “reference” run in the present study:

Reference Run:

$$\begin{aligned}
 [C_1]_0 &= 8.8 \text{ mol/kg mixture} \\
 [W]_0 &= 0.16 \text{ mol/kg, } [A_1]_0 = 0 \text{ (feed of pure caprolactam and water)} \quad (6) \\
 \overline{DP}_d &= 140, [C_2]_d = 0.01 \text{ mol/kg, } t_f = 10 \text{ h}
 \end{aligned}$$

where the subscript 0 indicates feed conditions. Figure 1 shows how the temperature profile changes from iteration to iteration when the starting (assumed) profile is isothermal at 260°C. It is observed that the profile is essentially unchanged after about 30 iterations. It was found that, even though a faster convergence to the final optimal temperature profile can be achieved by increasing ϵ (Table III), numerical instabilities arise in some cases. The value of ϵ of about 0.001 gives a good blend of speed of convergence and numerical stability. Figure 2 shows how $\overline{DP}(t_f)$ and $[C_2](t_f)$ attain the desired values \overline{DP}_d and $[C_2]_d$ and how the unreacted caprolactam increases as the number of iterations is increased. It may be mentioned^{28–31} that the control-vector iteration method used in this study converges relatively slowly after the first few iterations and, usually, one combines this technique with faster converging second-order numerical techniques after these first few sets of computations. However, this was not felt necessary at this stage of study. The second point to note from Figure 2 is that it is not possible to attain a $\overline{DP}(t_f)$ of exactly 140 simultaneously with a $[C_2](t_f)$ of 0.01 exactly. This is possibly due to the effect of some amount of coupling of these variables. The deviations of $\overline{DP}(t_f)$ and $[C_2](t_f)$ from the desired values are small, however.

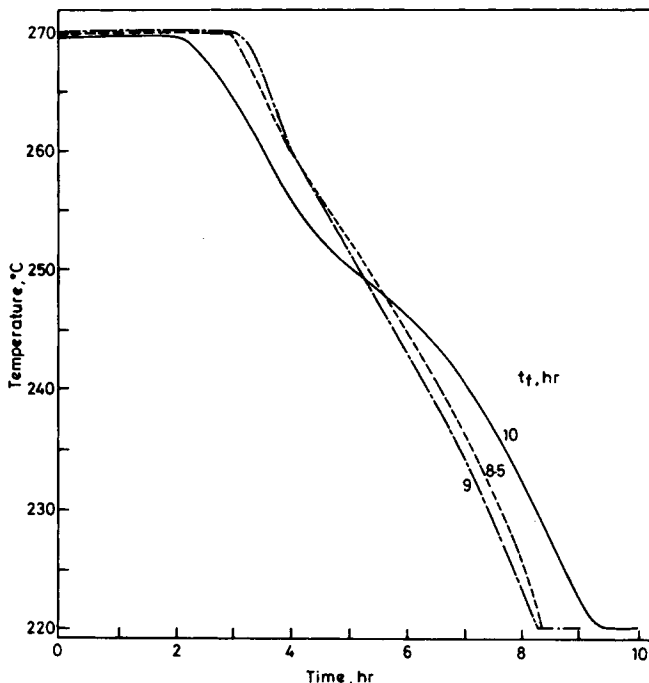


Fig. 7. Effect of t_f on the optimal temperature profile (---) $t_f = 8.5$ h, $\overline{DP}(t_f) = 140.51$, $[C_2](t_f) = 0.01$ mol/kg, conversion (t_f) = 75.47%; (-.-) $t_f = 9$ h, $\overline{DP}(t_f) = 140.93$, $[C_2](t_f) = 0.00995$ mol/kg, conversion (t_f) = 75.51%; (—) reference run, conversion (t_f) = 75.87%, $\epsilon = 0.0001$ – 0.002 .

The effect of the initial guess $T(t) = T_0$ is shown in Figure 3. The temperature profiles are found to be relatively insensitive to the choice of T_0 . A slight numerical instability (in terms of a local drop in temperature) is observed for the case when T_0 is 265°C . Similar local temperature drops were also observed for larger values of ϵ than 0.0013 for $T_0 = 260^\circ\text{C}$. No attempt was made to get rid of this temperature instability since the aim of this figure was solely to illustrate the insensitivity of the final temperature profile, and particularly of the values of $\overline{DP}(t_f)$, $[C_2](t_f)$, and $[C_1](t_f)$ to the choice of T_0 . Such a behavior is characteristic of this optimization algorithm,²⁸ and Denn²⁹ states that this insensitivity of the objective function and the end point values to the final temperature profile is indeed a blessing in disguise for an engineer. In this paper, an isothermal initial profile with $T_0 = 260^\circ\text{C}$ is used for all runs hereafter. It may be added that second-order techniques, which are computationally and conceptually more difficult as well as sensitive to convergence problems, can, at times, give better results.

Figure 1 establishes that for optimal performance of the reactor, the temperature must be maintained high for the first few hours, and, thereafter, be reduced to near the lower value. A similar optimal temperature profile has been obtained by Mochizuki and Ito.²⁴ This type of a profile is in marked contrast to that reported earlier,²⁵ where the objective function was more of relevance to a designer of a new reactor. Comparisons with the profile of Mochizuki and Ito cannot be attempted since only semiquantitative results have been presented by these workers. Differences in the behavior between the present profiles and those obtained by Mochizuki and Ito can be attributed to the use of different kinetic schemes for cyclic dimer formation.

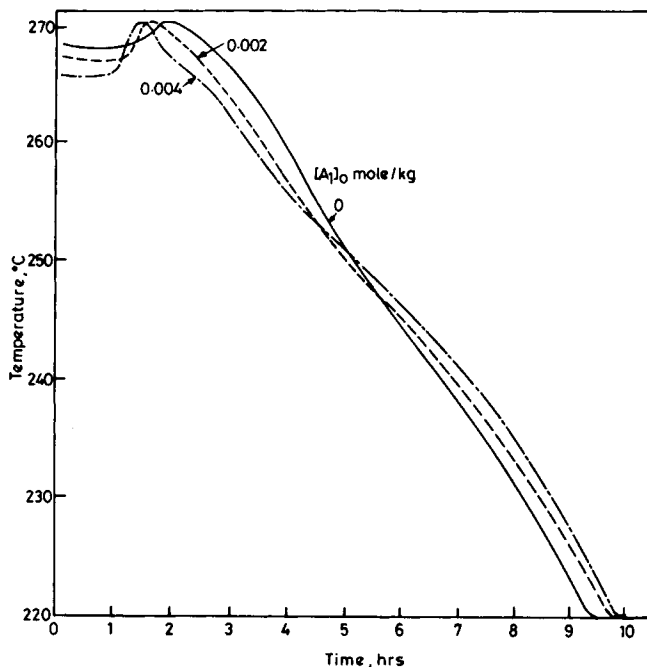


Fig. 8. Effect of adding stabilizer A_1 to the feed (---) $[A_1]_0 = 0.002$ mol/kg, $\overline{DP}(t_f) = 140.73$, $[C_2](t_f) = 0.00989$, conversion (t_f) = 76.52%; (-.-) $[A_1]_0 = 0.004$ mol/kg, $[C_2](t_f) = 0.01014$, conversion = 77.58%, $\overline{DP}(t_f) = 140.04$; (—) reference curve. Initial trial temperature = 255°C for all cases; $\epsilon = 0.0001$ –0.002.

Having established the effect of some of the *computational* parameters e. g., ϵ , T_0 , iterations, etc., the effect of design variables can now be studied. The effect of \overline{DP}_d is shown in Figure 4. It is observed that higher temperatures are required over the middle section of the reactor while lower temperatures are required near the end in order to obtain $\overline{DP}(t_f)$ of 145, keeping $[C_2](t_f)$ fixed at 0.01. In order to obtain convergence for \overline{DP}_d of 145, $[C_2]_d = 0.01$, we had to vary the value of ϵ with the number of iterations, using an interactive computer terminal, such that at no stage the change in temperature at any position exceeded 5°C. Similar results for $\overline{DP}_d = 135$, $[C_2]_d = 0.01$ could not be obtained since both these constraints could not be satisfied simultaneously.

The effect of $[C_2]_d$, keeping \overline{DP}_d fixed at 140, on the optimal temperature profile is shown in Figure 5. A lower requirement of the cyclic dimer concentration forces the temperature to be lower over most of the length of the reactor. Once again convergence could not be attained for the case of $[C_2]_d = 0.0105$, $\overline{DP}_d = 140$. The two end-point constraints, therefore, can be decided only within a certain range because of the coupling of the equations.

Figure 6 shows how a higher concentration of water in the feed requires lower temperatures over most of the reactor length, to achieve the same \overline{DP}_d and $[C_2]_d$. Again, these two end-point constraints could not be independently satisfied at higher values of $[W]_0$ of 0.180 mol/kg.

Figure 7 shows how the optimal temperature profile varies when the residence time t_f is changed from 10 h to 8.5 h. It is seen that one must maintain higher temperatures in the initial half of the reactor length if one wishes to obtain the same product in a shorter residence time. It has been deduced earlier²⁵ that the

degree of polymerization is controlled to a large extent by the temperature in this zone. In contrast, a lower temperature is necessary in the second half of the reactor length because $[C_2](t_f)$ is controlled by the temperature in this region. It is observed that the final polymer has about the same $\overline{DP}(t_f)$ and $[C_2](t_f)$ in all three cases, though the conversion of the monomer increases marginally with t_f . Thus, this figure shows that there exists some sort of a global optimum for a given feed wherein the residence time t_f is also the lowest.

Figure 8 shows the effect of adding small amounts of a monofunctional acid stabilizer to the feed. It is known that the addition of such stabilizers speeds up the conversion, but simultaneously lowers the \overline{DP} of the product. Thus, in order to get the same value of $\overline{DP}(t_f)$, it is intuitively expected that higher temperatures will be required. This figure shows this to be so over a substantial portion near the end of the reactor. What is interesting is that, in this case, the final conversion of the caprolactam is higher when the value of $[A_1]_0$ is larger. This behavior is in marked contrast to the results obtained by varying the other independent variables (even though the effect is not too pronounced). An interesting possibility would be to decrease the feed water concentration and increase $[A_1]_0$ in order to get higher final conversions keeping $\overline{DP}(t_f)$ and $[C_2](t_f)$ fixed, and then obtain global optimum conditions. However, such a study would have to be done using search techniques rather than analytically.

It may be added that several other values of \overline{DP}_d and $[C_2]_d$ were tried, and different optimal temperature profiles were obtained. In one case where $\overline{DP}_d = 100$, $[C_2]_d = 0.012$ mol/kg, and $[W]_0 = 0.44$ mol/kg, the optimal temperature profile came out as monotonically increasing from about 238°C to 245°C. However, such low molecular weights of nylon 6 are usually not of commercial importance, and so results for these are not being presented.

CONCLUSIONS

A detailed parametric study has been made of the optimal temperature profiles in nylon 6 polymerization with end-point constraints. An objective function similar to that used by Mochizuki and Ito²⁴ has been used, along with his end constraints. However, the kinetic scheme is more precise, and quantitative results have been presented. The results obtained are in accord with intuitive expectations if we realize that the temperature in the initial region of the reactor controls the degree of polymerization more significantly while that near the end controls the cyclic dimer concentration. Global optimal reactor design is now possible using various search techniques, with $[A_1]_0$, t_f , and $[W]_0$ as additional independent variables.

References

1. P. H. Hermans, D. Heikens, and P. F. Van Velden, *J. Polym. Sci.*, **30**, 81 (1958).
2. F. Wiloth, *Z. Phys. Chem.*, **5**, 66 (1955); **11**, 78 (1957).
3. Ch. A. Kruissink, G. M. Vander Want, and A. J. Staverman, *J. Polym. Sci.*, **30**, 67 (1958).
4. H. K. Reimschuessel and K. Nagasubramanian, *Chem. Eng. Sci.*, **27**, 1119 (1972).
5. K. Tai, H. Teranishi, Y. Arai, and T. Tagawa, *J. Appl. Polym. Sci.*, **24**, 211 (1979).
6. K. Tai, H. Teranishi, Y. Arai, and T. Tagawa, *J. Appl. Polym. Sci.*, **25**, 77 (1980).
7. Y. Arai, K. Tai, H. Teranishi, and T. Tagawa, *Polymer*, **22**, 273 (1981).
8. K. Tai, Y. Arai, H. Teranishi, and T. Tagawa, *J. Appl. Polym. Sci.*, **25**, 1789 (1980).

9. K. Tai, Y. Arai, and T. Tagawa, *J. Appl. Polym. Sci.*, **27**, 731 (1982).
10. K. Tai and T. Tagawa, *J. Appl. Polym. Sci.*, **27**, 2791 (1982).
11. J. M. Andrews, F. R. Jones, and J. A. Semlyen, *Polymer*, **15**, 420 (1974).
12. M. Mutter, U. W. Suter, and P. J. Flory, *J. Am. Chem. Soc.*, **98**, 5745 (1976).
13. M. V. Tirrell, G. H. Pearson, R. A. Weiss, and R. L. Laurence, *Polym. Eng. Sci.*, **15**, 386 (1975).
14. S. K. Gupta, A. Kumar, P. Tandon, and C. D. Naik, *Polymer*, **22**, 481 (1981).
15. S. K. Gupta, C. D. Naik, P. Tandon, and A. Kumar, *J. Appl. Polym. Sci.*, **26**, 2153 (1981).
16. A. Ramagopal, A. Kumar, and S. K. Gupta, *Polym. Eng. Sci.*, **22**, 849 (1982).
17. S. K. Gupta, D. Kunzru, A. Kumar, and K. K. Agarwal, *J. Appl. Polym. Sci.*, **28**, 1625 (1983).
18. S. Mochizuki and N. Ito, *Chem. Eng. Sci.*, **33**, 1401 (1978).
19. K. Nagasubramanian and H. K. Reimschuessel, *J. Appl. Polym. Sci.*, **16**, 929 (1972).
20. S. K. Gupta, A. Kumar, and K. K. Agarwal, *J. Appl. Polym. Sci.*, **27**, 3089 (1982).
21. K. Nagasubramanian and H. K. Reimschuessel, *J. Appl. Polym. Sci.*, **17**, 1663 (1973).
22. P. J. Hoftyzer, J. Hoogschagen and D. W. van Krevelen, Proc. 3rd Eur. Symp. Chem. Reaction Eng., Amsterdam, September 15-17, 1964, p. 247.
23. W. F. H. Naudin ten Cate, Proc. Intern. Conf. Use of Elec. Computers in Chem. Eng., Paris, April 1973.
24. S. Mochizuki and N. Ito, *Chem. Eng. Sci.*, **28**, 1139 (1973).
25. A. Ramagopal, A. Kumar, and S. K. Gupta, *J. Appl. Polym. Sci.*, **28**, 2261 (1983).
26. H. K. Reimschuessel, *J. Polym. Sci., Macromol. Rev.*, **12**, 65 (1977).
27. S. K. Gupta and A. Kumar, *Chem. Eng. Commun.*, **20**(1-2), 1 (1983).
28. W. H. Ray and J. Szekely, *Process Optimization*, 1st ed., Wiley, New York, 1973.
29. M. M. Denn, *Optimization by Variational Methods*, 1st ed., McGraw-Hill, New York, 1969.
30. L. Lapidus and R. Luus, *Optimal Control of Engineering Processes*, Blaisdell, Waltham, Mass., 1967.
31. A. E. Bryson and Y. C. Ho, *Applied Optimal Control*, Blaisdell, Waltham, Mass., 1969.

Received May 28, 1983

Accepted November 16, 1983